



Some Mineralogical Approaches to Study the Biocarbonate and the Carbonate-Siliceous Nodules

Liubov V. Leonova, Akhmet A. Galeev, Yulia S. Simakova,
Alena S. Ryabova, Liudmila Yu Kuzmina, Stepan P. Glavatskikh
and Olga Ya Cherviatsova

Abstract Nodules of different compositions from Paleozoic sedimentary rocks and those deposited by microbial communities in laboratory-scale experiments were studied by the use of electron paramagnetic resonance, X-ray diffraction, and scanning electron microscopy with energy-dispersive spectrometer. The study of the mineral composition of fossil nodules showed that they have monomineral composition of dolomite or chalcedony, mixed composition of dolomite-chalcedony or of opal-dolomite, and finally nodules can be composed of alternating opal and chalcedony layers cementing fine dispersed dolomite grains or clusters of irregular shape. Similarity in dolomite crystal lattice defects in both the nodules and the host rocks confirms their formation during syndimentary early diagenesis. Bacterial activity during sedimentary nodules growth is evidenced by the presence of paramagnetic carbon-centered free radicals of fossilized protein substances and findings of fossil bacteria. Experimental laboratory-scale modeling of natural carbonate deposition by microbial communities confirms that bacteria can promote nodules formation.

L.V. Leonova (✉) · S.P. Glavatskikh
Institute of Geology and Geochemistry, Ekaterinburg, Russia
e-mail: lvleonova@yandex.ru

A.A. Galeev
Institute of Geology and Petroleum Technologies, Kazan Federal University, Kazan, Russia
e-mail: akhmet.galeev@kpfu.ru

Y.S. Simakova
Institute of Geology of the Komi Science Center, Urals Branch of RAS, Syktyvkar, Russia
e-mail: yulia5-07@mail.ru

A.S. Ryabova · L.Y. Kuzmina
Institute of Biology, Ufa Scientific Center of RAS, Ufa, Russia
e-mail: ljku@anrb.ru

O.Y. Cherviatsova
Shulgan-Tash State Nature Reserve, Irgizly Village, Republic of Bashkortostan
e-mail: kittary@yandex.ru

22 **Keywords** Nodules • Bacterial activity • Biogenic carbonates and flints • Methods
23 of investigation • Experiments

24
25 Sedimentary and volcanic-sedimentary rocks are formed in the water-saturated
26 upper part of the lithosphere. Water-saturated conditions can be considered to be the
27 most favorable for biogenic–abiogenic interaction when the biota affects both
28 upwelling gas–fluid flows from the Earth’s interior and surface deposits resulting in
29 the formation of biominerals. Current reassessment of the role of bacterial assem-
30 blages in sedimentogenesis and lithogenesis creates a new direction in the lithology
31 called as “bacterial lithogenesis” (Antoshkina 2012). Since almost all sedimentary
32 rocks formed in varying degrees with the participation of the microbiota, one of the
33 tasks of lithogenesis is to develop models of sedimentation in ancient epicontinental
34 basins taking into consideration the essential role of bacterial factor. The study of
35 nodules can be useful for solving these tasks. The problem is that the participation
36 of bacteria in sedimentogenesis and lithogenesis should be proved using a complex
37 of physical research techniques.

38 Lithological syngenetic nodules are often found in sedimentary rocks of different
39 geological age formed in various facies conditions. Chemical and mineral composi-
40 tions of the nodules and the surrounding rock may be the same or different from
41 one another: carbonates, phosphates, silica oxides (opal, chalcedony, quartz),
42 oxide-hydroxides of iron and manganese, and mixed iron-manganese oxides. There
43 are microscopic and giant, monomineralic or mixed mineral nodule, including clays
44 and sandstones. Often, nodules are spheroid or disk-shaped but sometimes form a
45 variety of more complex shapes. Nodules of similar shape but of different mineral
46 composition are presented in our collection (Fig. 1a–f): a dolomite (gypsum-
47 dolomite stratum P₂ kz₂, right bank of the Volga river, v. Klyuchischi); b vernadite-
48 lithiophorite-quartz mineral association (jasper-silicite deposits with man-
49 ganese ore interlayers D₂ ef, Southern Urals, Baimaksky district, v. Fayzulino);
50 c sandstone with quartz cement (jasper-silicite deposits D₂ ef-zv, Southern Ural,
51 Chelyabinsk region, v. Kizilskoe); d opal-dolomite association (gypsum-dolomite
52 deposits P₂ kz₂, right bank of the Volga river, v. Krasnovidovo); e gray jasper
53 (jasper-silicite deposits D₂ ef-zv, Southern Ural, Sibai); f quartz sandstone with
54 vernadite-lithiophorite cement (jasper-silicite complex D₂ zv, Southern Ural, Sibai
55 district, v. Khasanovo).

56 Outcrops of the nodules occur locally in the vertical section of a given sedi-
57 mentary horizon, forming meadows in landscape views, and often traced from one
58 layer to another. Their presence indicates local geological events in paleobasin
59 development—localized gas/fluid flow associated with seafloor seeps. However, the
60 question of the nodules genesis up to this time predominates the model of che-
61 mogenic consolidation in the late diagenesis and catagenesis, implying the presence
62 of permeable media and migrating solutions with a high degree of mineralization

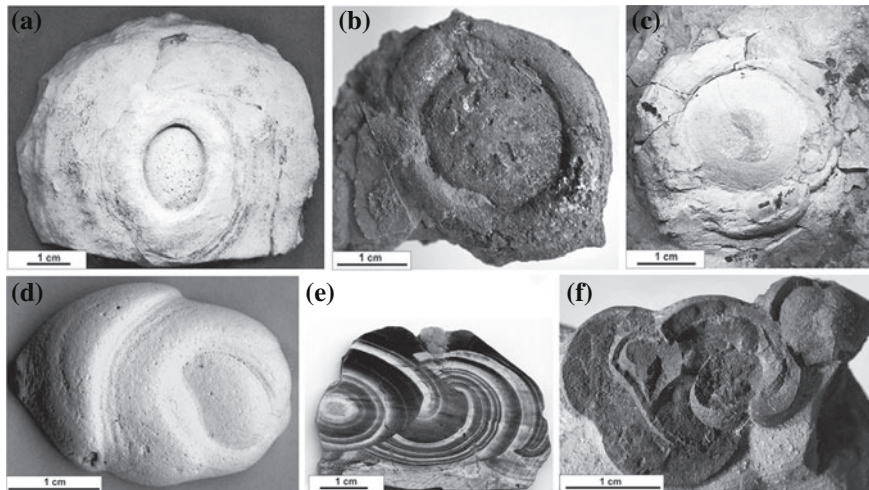


Fig. 1 a–f Nodules with similar morphology and differing in mineral composition: **a** dolomite (gypsum-dolomite stratum P₂ kz₂, right bank of the Volga river, v. Klyuchischi); **b** vernadite-lithiophorite-quartz mineral association (jasper-silicite deposits with manganese ore interlayers D₂ ef, Southern Urals, Baimaksky district, v. Fayzulino); **c** sandstone with quartz cement (jasper-silicite deposits D₂ ef-zv, Southern Ural, Chelyabinsk region, v. Kizilskoe); **d** opal-dolomite association (gypsum-dolomite deposits P₂ kz₂, right bank of the Volga river, v. Krasnovidovo); **e** gray jasper (jasper-silicite deposits D₂ ef-zv, Southern Ural, Sibai); **f** quartz sandstone with vernadite-lithiophorite cement (jasper-silicite complex D₂ zv, Southern Ural, Sibai district, v. Khasanovo)

63 (Strakhov 1962). But this model cannot explain the genesis of those nodules which
 64 are the same in the mineral composition with surrounding rocks, or whose specific
 65 shapes (Fig. 1a–f) do not follow the mechanism of chemogenic consolidation.

66 An alternative hypothesis of the dissolved substances concentration and of
 67 forming consolidated nodules is related to the leading role of microbial commu-
 68 nities, the part of which can promote mineral precipitation (Berner 1971; Skinner
 69 and Fitzpatrick 1992; De Craen et al. 1999; Green and Madgwick 1991; Tazaki
 70 2000; Raiswell 1976; Stocks et al. 1999). This is supported by the findings of
 71 mineralized remains of the fossil cyanobacteria and the bacteria buried in nodules
 72 substrate. Unfortunately, in carbonate formations such finds are rare. Therefore, this
 73 paper focuses on the study of carbonate nodules. Probably, the depositions of such
 74 mineral aggregates are biochemogenic in nature and occur as a result of catalytic
 75 influence of bacterial activity. In these cases it is necessary to adapt the analytical
 76 research techniques used in the physics and chemistry of minerals, which may
 77 reveal the implicit role of bacteria in concretion formation. And of course, the
 78 experimental evidences are the best way to prove the hypothesis.

1 Materials

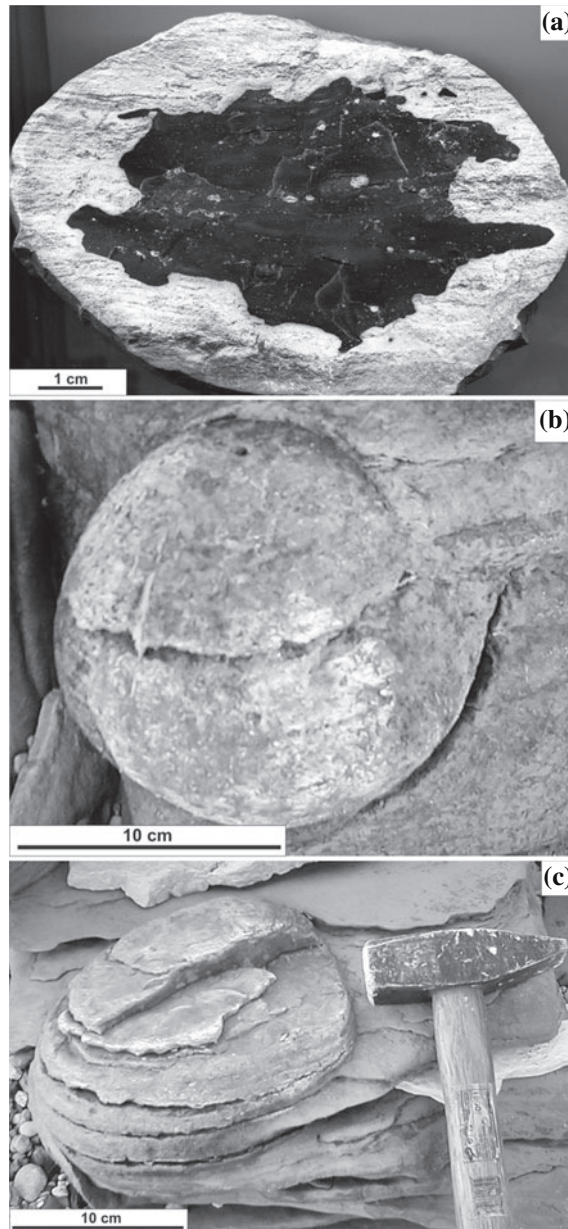
For this study, we collected 40 samples from gypsum-dolomite Upper Permian (P_2 kz_2) deposits on the right bank of the Volga river (Russia, the western part of the Republic of Tatarstan, 50–100 km downstream of Kazan: Pechischi, Krasnovidovo, Antonovka, Yashelcha, Tenishevo piers) (Fig. 2). The carbonate sediments, formed in the shallow marine-salinated basin, are dominating this area. The brachyanticlinal uplift and the small folds characterize the structural features of this area, but the rocks show no signs of regional metamorphism, inheriting the outlines of the relief on the roof of the Upper Devonian (Geology 2007). However, some local changes of the rocks due to the penetration of hydrocarbon fluids are observed in the vicinity of brachyanticlinal uplifts (Syukeevskoe, Kama-Ustyinsky, Krasnovidovskoe, Verkhneuslonsky, Sviazhsky at alias) (Geology 2007; Korolev et al. 2014).

Nodules in the outcrops occur at several stratigraphic levels of upper Kazanian horizon: Prikazanskaya, Pechishchinskaya, Verkhneuslonskaya, and Morkvashinskaya stratas (Geology 2007). They are composed of dolomite, silica, dolomite-silica (chalcedony) or dolomite-opal. Moreover, silica (chalcedony) appears in different forms: fine-dispersed, lumpy, or localized in the nucleation center of nodules (Fig. 3a). The color of the silica component of gray or black depends on ultrafine and nano-sized inclusions of pyrite (melnikovite), magnetite, and maghemite. The maximum size of up to 60 cm is typical to purely dolomite nodules, whereas the dolomite-opal nodules are of the minimum size of 1–3 cm. The dominating shapes are spheroids (Fig. 3b) or flattened spheroids (Fig. 3c), rarely—spheroids with rim (Fig. 1a).



Fig. 2 Survey maps of studied area

Fig. 3 a–c Nodules from *right* bank of the Volga river, v. Krasnovidovo:
a chalcedony component is localized in the central part of dolomite concretion;
b spheroidal dolomite concretion in dolostone;
c flattened-spheroidal dolomite concretion in dolostone



2 Methods

In this study, we used the following physical techniques:

- electron paramagnetic resonance (EPR) (spectrometer EPR-PS100.X operating at 9.772 GHz), used to reveal the remains of fossil organic matter in mineral matrices of concretions, and to study point defects in crystal structure (radiation centers) of carbonate minerals of host rocks and nodules;
- experimental laboratory-scale modeling of natural biocarbonate deposition by microbial communities;
- scanning electron microscopy (SEM) (JSM-6390LV JEOL) with energy-dispersive spectrometer (EDS—Inca Energy 450), used to study mineral aggregates and microfossils micromorphology, and to determine the chemical composition of the minerals. The fractured and polished surfaces of samples were carbon coated for microscopic purposes.
- powder X-ray diffraction (XRD) (X-ray Diffractometer Shimadzu XRD-6000, CuK α , Ni filter, 30 kV, 20 mA, scanning in 2θ range from 02° to 35° and from 15° to 55°), used to characterize the crystal structure determination of mineral composition of nodules and microbial carbonates, deposited in laboratory.

3 Justification of Selected Methods

A prerequisite for the use of EPR technique in our work were the previously obtained spectral characteristics of carbon radicals in organic matter (OM) for the most common fossil residues of different age, genesis, and manifestation forms in the sedimentary rocks (Votyakov et al. 2005; Murav'yev 2007; Soroka et al. 2007; Conard 1984). Depolymerization and repolymerization products of proteins, lignin, and cellulose, such as fragments of aminoacids and polysaccharides, usually contain uncompensated bonds which can be locally stabilized in the form of carbon-centered free radicals (R_C -org) with paramagnetic properties. Being fossilized, these radicals can be preserved within the mineral matrix for a long period of geological time (Votyakov et al. 2005). The concentration of these paramagnetic centers in fossils can be changed during the specific heat treatment in laboratory conditions (Fig. 4a). The characteristic parameters of their EPR spectra are the g -value, the line width (ΔH , mT), and the line shape (mainly Lorentzian).

By measuring the paramagnetic properties and their temperature dependence, one can distinguish the following types of fossil OM:

- humus-sapropel matter metamorphized at early stages of diagenesis. EPR spectra with $g \sim 2.0031$ and $\Delta H \sim 0.5 \div 0.9$ mT are observed in the raw samples and gradually disappear when treated up to 350 °C (Fig. 4b).

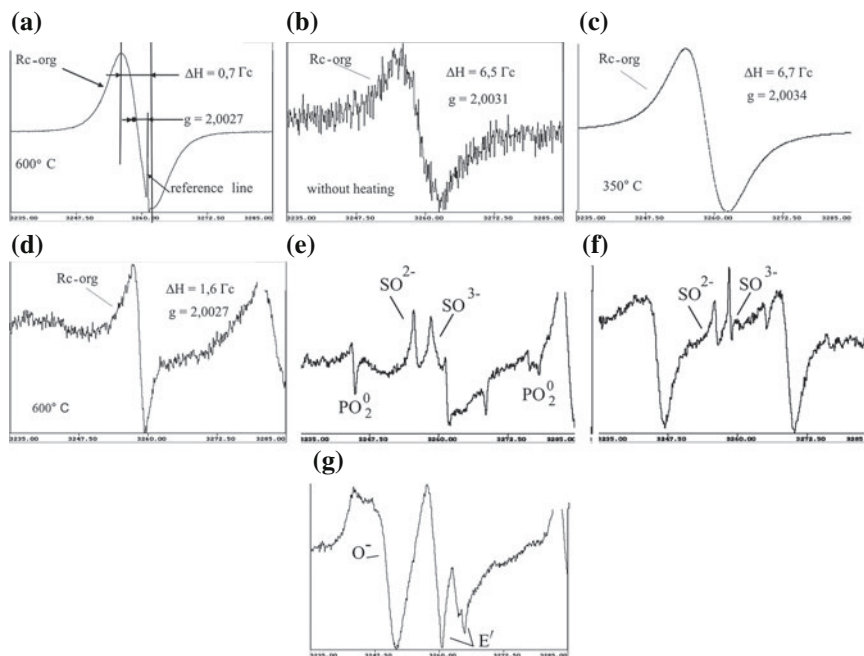


Fig. 4 a–g EPR spectra in the range of radical lines: **a** characteristics of the resonance lines in spectrum of carbon-centered organic free radicals $R_C\text{-org}$ (g -factor is a dimensionless parameter, defining the Zeeman splitting of spin multiplets for a given atoms, ΔH —line width in mT (~ 10 Gs), and the upper temperature limit of stability range for paramagnetic properties of radicals); **b** typical $R_C\text{-org}$ EPR spectrum ($g \sim 2.0031$, $\Delta H \sim 0.5 \div 0.9$ mT) of the humus-sapropel organic matter which is observed in the raw sample and disappears after heat treatment; **c** $R_C\text{-org}$ spectrum of fossil OM of plant origin ($g \sim 2.0030 \div 2.0038$, $\Delta H \sim 0.4 \div 0.7$ mT, 350°C); **d** typical $R_C\text{-org}$ EPR spectrum of organic residues of animal, including bacterial, protein (collagen) ($g = 2.0027 - 2.0028$, $\Delta H \approx 0.5 \div 0.4$ mT, upper temperature limit of stability range is 600°C); **e** radiation centers SO_2^- , SO_3^- , PO_2^0 in dolomite; **f** radiation centers SO_2^- , SO_3^- in calcite; **g** radiation centers O^- и E' in silica components

- 139 • plant matter (lignin, cellulose). EPR spectrum with $g \sim 2.0030 \div 2.0038$ and
140 $\Delta H \sim 0.4 \div 0.7$ mT can be observed in the raw samples and gradually increases
141 when treated with maximum intensity at 350°C and then disappear (Fig. 4c).
- 142 • OM of animal origin (collagen), including bacteria, is characterized by EPR
143 spectra with— $g = 2.0027 - 2.0028$, $\Delta H \approx 0.05 \div 0.4$ mT, which disappears at
144 treatment above 600°C (Fig. 4d).

145 At high degree of natural coalification of OM, all the above-mentioned signals
146 $R_C\text{-org}$ can be observed in raw samples and disappear when treated to 350°C or
147 600°C depending on the original nature (Murav'yev 2007; Khasanov and Galeev
148 2008; Conard 1984).

149 The presence of radiation paramagnetic centers in the EPR spectra of minerals
150 indicates that these minerals were not subjected to recrystallization because defect

151 structure of minerals is unique for a given sediment's formation conditions.
152 Similarity in a set of radiation paramagnetic centers for nodules and surrounding
153 rocks may indicate their syngenetic origin.

154 The sedimentary carbonate rocks contain relatively minor quantities of
155 radioactive constituents in comparison with others. The detectable concentration of
156 radiation-induced defects in crystal lattice of carbonate minerals may appear only in
157 the early stages after deposition, before burial compaction, due to the influence of
158 cosmogenic radioisotopes dissolved in shallow marine or pore waters. Primarily,
159 the radiation-induced defects appear as metastable recharging of host lattice ions
160 CO_3^- , CO_3^{3-} , and in part CO_2^- . Over geological time, these excess charges are
161 redistributed in lattice and accumulated in the vicinity of impurities to form radicals
162 SO_2^- , SO_3^- , PO_2^{2-} (or PO_2^0), and CO_2^- (Fig. 4e and f), which are commonly
163 observed in Mesozoic, Paleozoic, and Proterozoic carbonates. For silica oxide
164 minerals there are well-known radiation-induced centers related with oxygen ions
165 O^- and E' (Fig. 4g).

166 Experimental laboratory-scale modeling of natural biocarbonate deposition by
167 microbial communities allows one to study not only the stability of community
168 structure itself and pure cultures of bacteria, but also to estimate their role in
169 carbonate deposition. As a primer, we used natural microbial community, combined
170 with the habitat of various geo ecosystems from Shulgan-Tash cave (State Nature
171 Reserve, Republic of Bashkortostan, Irgizly village). The aim of the experiment
172 no. 1 was to identify the nutrient media, the most favorable for the development of
173 bacterial communities and carbonate deposits. A Petri dish with bacterial colonies
174 on an agar-based growth medium Variant 3 were inoculated by mineral pieces of
175 needle-fiber (NFC), pool fingers (lake aggregates of calcite), and soil from the cave
176 hall "Raduzhny" where gypsum crystals are growing. The most productive variants
177 of culture media were used for the following experiments. Experiment no. 2 was
178 conducted to study the newly formed biocarbonates and possible intermediate
179 phases by the use of analytical research techniques: SEM, EDS, and XRD.
180 Microbial isolates for this series of experiments were grown in medium variant 3
181 (Danielli and Edington 1983), g/l (modified): KNO_3 (0.5); $\text{Na}_2\text{HPO}_4 \cdot 12\text{H}_2\text{O}$ (0.25);
182 Ca succinate (5.0) (succinic acid (3.54); $\text{CaCl}_2 \cdot 2\text{H}_2\text{O}$ (3.3)); Oxoid agar (15.0); pH
183 7.1, and also in Grans medium (Mason-Williams 1969) g/l (modified): Ca malate
184 (5.0) (malic acid (4.02); $\text{CaCl}_2 \cdot 2\text{H}_2\text{O}$ (3.3)); KNO_3 (0.5); $\text{Na}_2\text{HPO}_4 \cdot 12\text{H}_2\text{O}$ (0.25);
185 Oxoid agar(15.0); pH 7.2. The isolates were grown in the growth medium peptone
186 water g/l (modified) (Antipchuk 1979): Peptone (5.0); K_2HPO_4 (1.0); KH_2PO_4
187 (1.0); $\text{MgSO}_4 \cdot 7\text{H}_2\text{O}$ (0.5); CaCl_2 -3; NaCl a very small content, were studied only
188 by XRD.

189 The samples were prepared as follows: microbial community and isolates were
190 plated on solid culture media (the crops for XRD were duplicated in liquid media)
191 and cultured for 30 days. The specimens were prepared from these substrates
192 including the spent culture medium with biofilm and the crystalline phase of newly
193 formed carbonate minerals of different dimensions.

194 The substrate was dried at a temperature not higher than +25 °C and then the
195 piece cut out film with crystals was mounted on carbon adhesive tape and placed in



196 vacuum coating systems for SEM. To study the newly formed carbonates by XRD,
197 the bacterial biomass were scraped from the culture media and frozen in eppendorf
198 polypropylene tubes at -30°C . Grown in liquid media carbonates and microbial
199 biomass were centrifuged at 5000 rpm and then frozen for transport to XRD lab-
200 oratory. It is assumed that in this manner the transformation of uncontrolled
201 hydrocarbonate into carbonate will proceed slowly that allows to reveal all the
202 phases of the newly formed carbonates. Unoriented samples for XRD analyses were
203 prepared by drying the gel on rectangular glass plates. Directly before the analytical
204 procedure ethyl alcohol was added to the glass slide with the sample for accelerated
205 drying.

206 **4 Results**

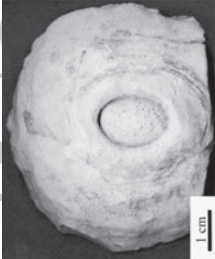
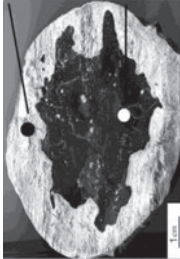
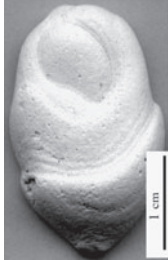
207 The study of the mineral composition of fossil nodules showed that they can have
208 monomineral composition of dolomite or chalcedony, mixed composition of
209 dolomite-chalcedony or of opal-dolomite, and finally nodules can be composed of
210 alternating opal and chalcedony layers cementing fine dispersed dolomite grains or
211 clusters of irregular shape.

212 **5 Electron Paramagnetic Resonance**

213 The results of the EPR study are present in Table 1 for the samples of most
214 representative mineral associations:

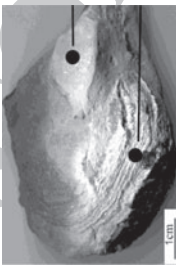
215 No. 1—dolomite, no. 2—black chalcedony concentration in middle of the
216 dolomite concretions, no. 3—opal-dolomite mineral association, and no. 4—black
217 pure chalcedony in dolomite host rock. EPR spectra of radiation centers SO_2^- ,
218 SO_3^- of dolomite are registered both in nodules and host rocks, the similar pattern
219 observed for E' centers of chalcedony. This indicates that the investigated objects
220 were formed together with surrounding rocks, and never were subjected to
221 recrystallization during diagenesis and regional metamorphism in subsequent
222 periods. Furthermore, the signals $R_{C\text{-org}}$ with $g = 2.0027$, $\Delta H \approx 0.14\text{--}0.16$ mT,
223 typical for nonmetamorphized residual organic matter of animal protein (collagen),
224 occur in EPR spectra only after treatment at 600°C , and there were no any spectra
225 registered which can be related with metamorphized OM, as well as with
226 humus-sapropel or plants matters. It should be noted that measured concentration of
227 paramagnetic centers $R_{C\text{-org}}$ in concretion was sometimes considerably higher than
228 in host rock. The well-preserved fossil OM within mineral matrices can be the
229 evidence of high mineralization speeds and microbial activity during concretion
230 growth because no faunal remains were found neither in concretions or in nearby
231 host rocks.

Table 1 EPR spectral characteristics of studied nodules

No.	Sample	Mineral composition	The presence of microfossils	The EPR characteristics of the signals in the field of radicals				
				Radiation centers		Radicals of organic carbon		
				E'	SO ₂ ⁻ SO ₃ ⁻	Without heating	350 °C	600 °C
1		Dolomite	-	+		-		+
2		Dolomite Black flint	- +	+ -		- -		+ +
3		Dolomite-opal	+	-		-		+

(continued)

Table 1 (continued)

No.	Sample	Mineral composition	The presence of microfossils	The EPR characteristics of the signals in the field of radicals					
				Radiation centers		Radicals of organic carbon			
				E'	SO ₂ ⁻ SO ₃ ⁻	Without heating	350 °C	600 °C	
4		The host rock dolomite Black flint	-	+	-	-	-	+	+

UNCORRECTED PROOF

232 6 Scanning Electron Microscopy

233 SEM and EDS analyses show that most nodules are composed by flocculant, drusy
 234 aggregations, and carbonate microcrystals (Fig. 5a) with a morphology different
 235 from rhombohedral grains of host rocks. Crystals and druses are characterized by
 236 similarity in size and by repeatability in shape. However, microbial fossils in the
 237 nodules are rare (Fig. 5b). Opal-dolomite nodules are always fine-grained mineral
 238 association, sometimes forming hollow spheroids (Fig. 5c), which possibly are
 239 mineralized remains of bacterial colonies.

240 Samples deposited in the laboratory experiment no. 1 contain carbonate
 241 crystals (Fig. 5d) similar in morphology to those in fossils or have a specific shape
 242 (Fig. 5e, f). There are crystals with biofilm on their surface (Fig. 5g).
 243 Microbial-induced precipitates form microscopic nodules (Fig. 5h and i). In
 244 experiment no. 2, we established that in pool fingers community, the abundance of
 245 microorganisms able to grow in media with organic acids (malic, succinic—Grans,

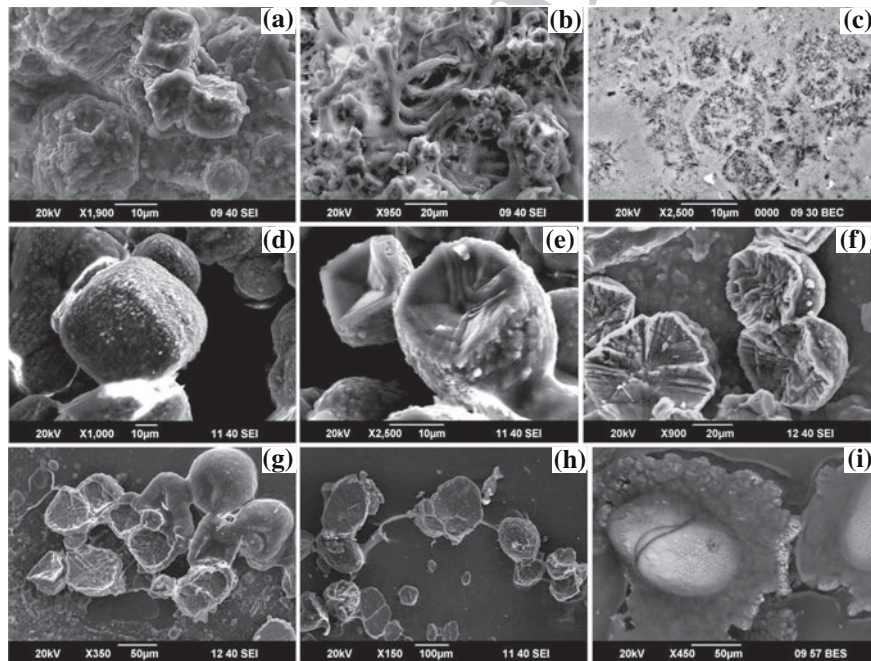


Fig. 5 a–i SEM images of carbonate nodules: **a** specific crystals of carbonates (dolomite and high-Mg-calcite) that constitute nodules in the Upper Permian deposits; **b** bacterial microfossils in the dolomite nodules; **c** microstructure in opal-dolomite nodules from the Upper Permian deposits; **d** bacterial controlled carbonate sediments in experiment No. 1; **e, f** bacterial controlled carbonate formation of a specific habitus, experiment No. 1; **g** subsequent stages of carbonate crystals encapsulation by biofilm, which deposits calcium carbonate; **h, i** carbonate microconcretions in experiment No. 1

Table 2 Colony of microorganisms selected to study the mineral sedimentation in bacterial mats

Strains	Culture media	The shape of the cell	Description colony: color, colony size	Color gram*	The consumption of glucose	Aerobic growth	The habit of the crystals, Plate 1
1-2a	Variant 3	Sticks	Colorless with yellow paint small colony	+	+	±	a
1-2b	Variant 3	Sticks	Colorless small colony	-	+	±	b
1-3	Variant 3	Cocci	Yellow large colony	-		+	c
1-3a	Variant 3	Cocci	Yellow small colony	+	+	+	d
1-4	Variant 3	Sticks	Colorless large butyrous colony	-	+	+	e
1-5	Variant 3	Cocci	Orange small colony	-	-	+	f
1-6	Variant 3 + peptone	Sticks	Colorless large butyrous colony	-	+	±	g
2-2	Grans medium	Sticks	Colorless large butyrous colony	-	-	±	h
2-5	Grans medium	Cocci	Yellow large colony	-	+	±	i
2-6	Grans medium	Sticks	Colorless large colony	-	+	+	j
2-7	Grans medium	Sticks	Colorless small colony	-	+	+	k

* Test: + Positive, - Negative, ± Optional gone anaerobic

variant 3, and variant 3 + peptone) was about $1.8 \div 4.6 \times 10^6$ KFU/g. From this broad microbial diversity after several passages and exceptions (loss of ability to precipitate minerals, pollution by fungi at alias), we studied the physiological and biochemical properties of the remaining 11 isolates in order to identify them and to estimate their ability to precipitate minerals. Selected cultures were represented by aerobes and facultative anaerobes, mainly of gram-negative rod-shaped bacteria (6 isolates) and of cocci (3 isolates), and only by two gram-positive isolates (Table 2). The difference in morphology of biominerals precipitated by different isolates was established from SEM analyses. The microscopic images of biocarbonate dominating forms are shown in plate (Plate 1a–l). The influence of nutrient medium on nodules morphology was negligible. As it is seen in Fig. 3, the different isolates 1–5 (Plate 1f), 2–5 (Plate 1i), 2–7 (Plate 1k) precipitate aggregations of similar morphology, even if the isolate 1–5 was cultivated on the medium Variant 3, whereas the isolates 2–5 and 2–7 on Grans medium (Table 2). When observed at high magnification (more than $\times 4300$), certain bacterial cells were found to be buried among crystal particles (Plate 1l).

7 X-ray Diffraction

XRD data indicate that calcite is the major crystalline component in sediments for all the analyzed samples. The amount of noncrystalline material (gel) evidenced by the XRD patterns of random mounts which exhibited high background levels and two humps with very broad maxima near 3.5 and 2.2 Å (Fig. 6). Nevertheless, distinct calcite peaks were detected on XRD patterns of such samples. As the gel in the samples dry, the calcite reflections on XRD patterns become more intensive and

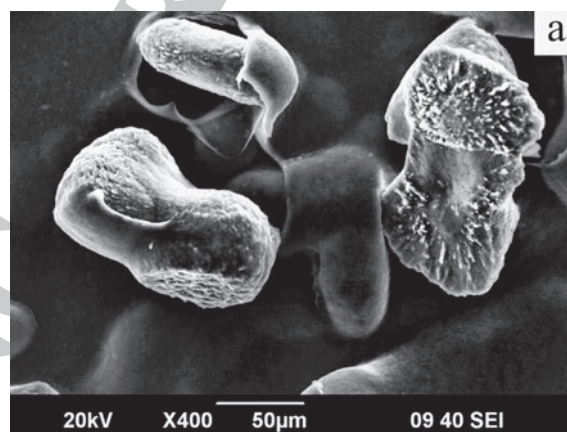


Plate 1 a–l SEM images of biocarbonate precipitates in experiment no. 2

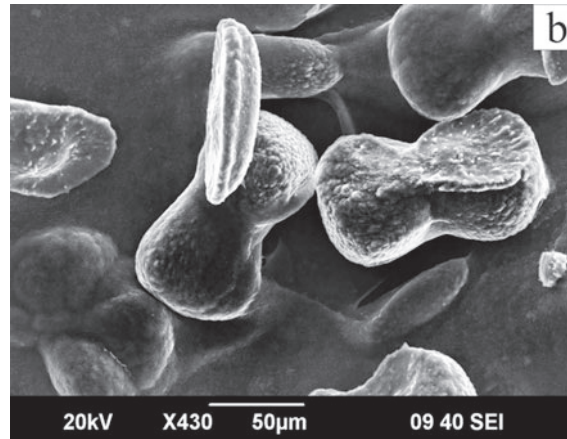


Plate 1 (continued)

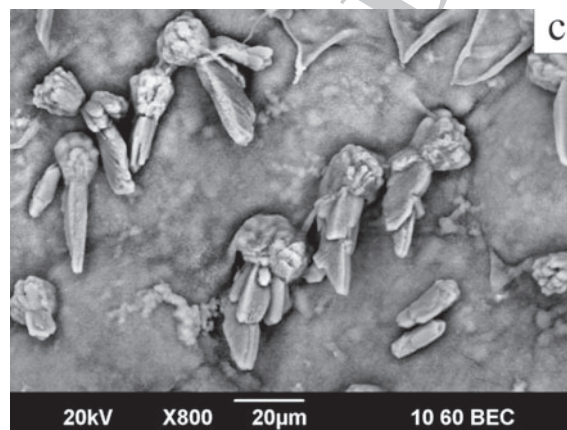


Plate 1 (continued)

269 narrow. Cell parameters have been determined for the biogenic calcites from the
 270 investigated samples (where possible, with Si as internal standard). Values of these
 271 parameters are very close to one another and have minimal deviations (Table 3).

272 It should be noted that in experimental precipitation induced by bacteria (Wei
 273 et al. 2011), the calcite was a dominant mineral phase. Some crystals after exper-
 274 imental interaction with bacteria had bacterial imprints on crystal surfaces. In spite
 275 of differences in the tasks of experiments, strains, and mediums chosen, calcite

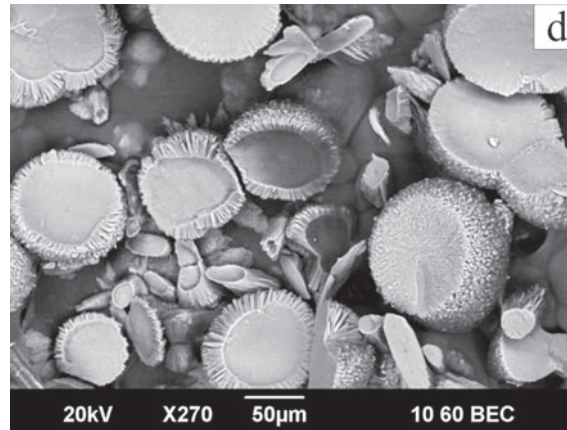


Plate 1 (continued)

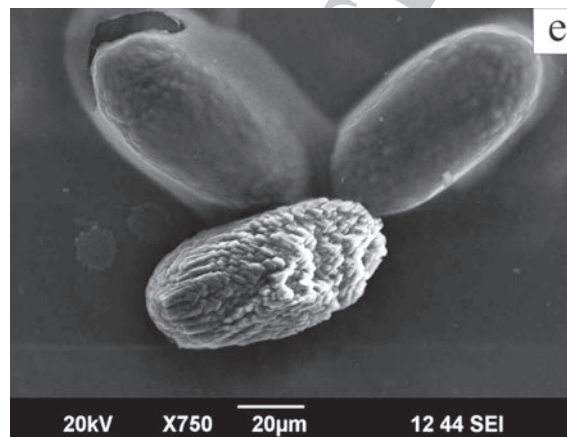


Plate 1 (continued)

276 precipitates regularly with increasing the pH of the medium. The presence of Mg
277 salts in the nutrient solution leads to the precipitation of Mg-calcite.

278 Presence of Mg-calcite was determined in the sample A formed on Peptone
279 nutrient solution ($\text{MgSO}_4 \cdot 7\text{H}_2\text{O}$ —0.5; CaCl_2 —3 g/l). Cell parameters of this
280 mineral are in good agreement with other data for biogenic Mg-calcite (sample A in
281 Table 3) (Bischoff et al. 1983; Paquette and Reeder 1990).



Plate 1 (continued)

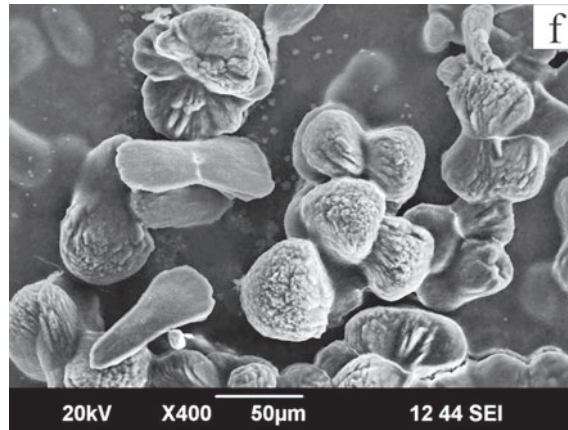


Plate 1 (continued)

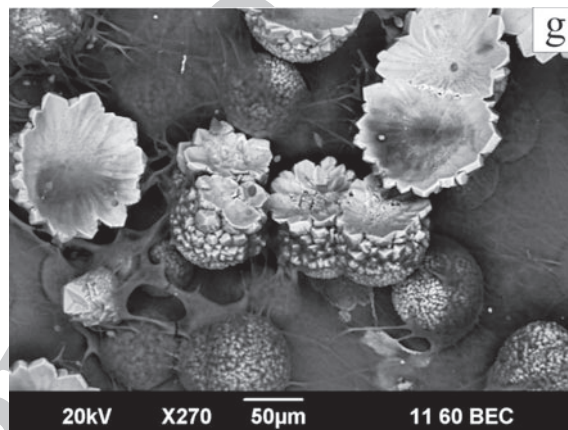


Plate 1 (continued)

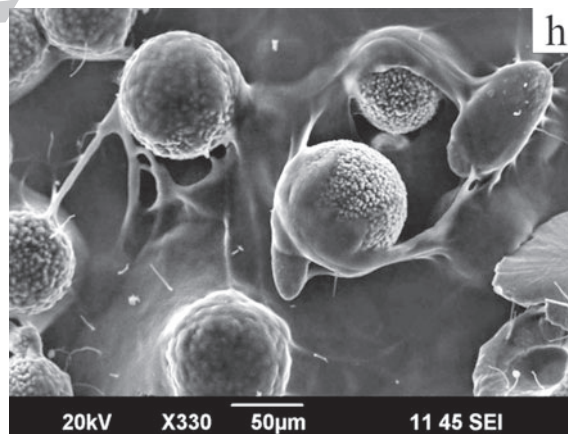




Plate 1 (continued)

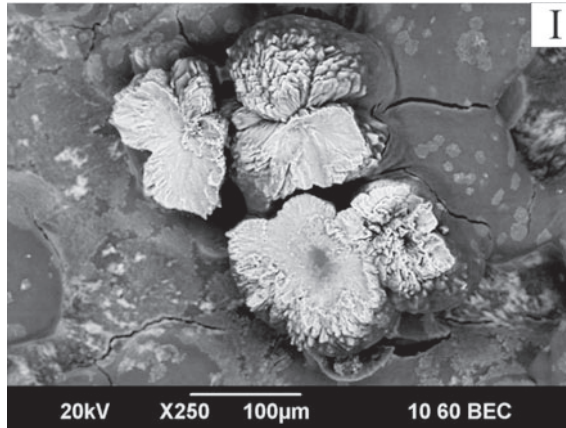


Plate 1 (continued)

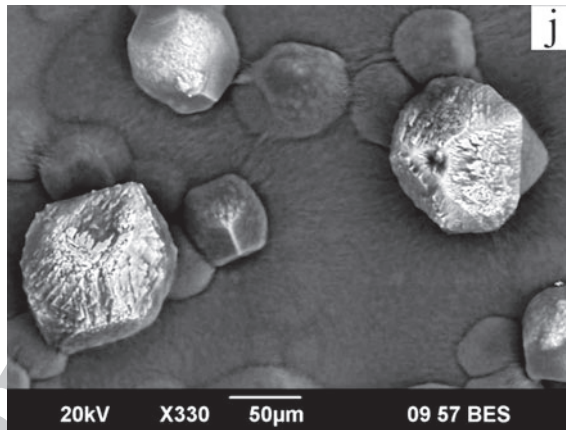
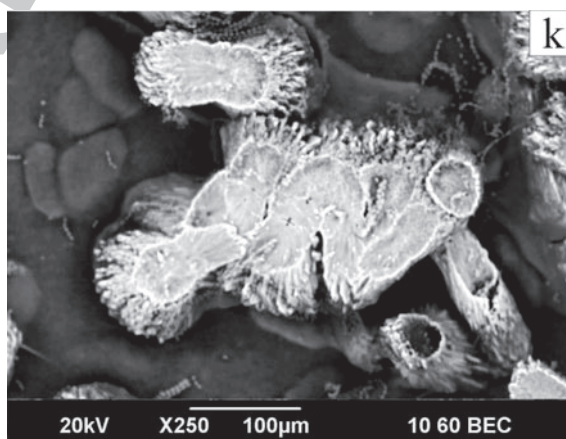


Plate 1 (continued)



UNCORRECTED

Plate 1 (continued)

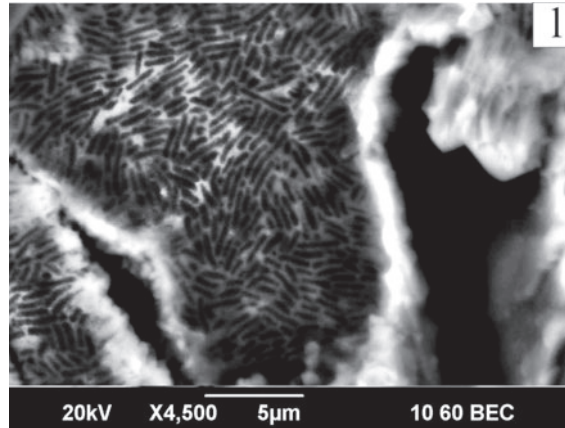
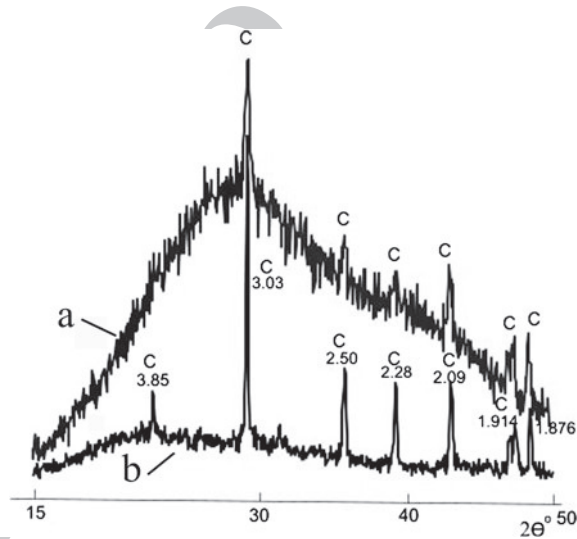


Fig. 6 X-ray diffraction patterns of sample 2–6: *a* gel state, *b* air-dried. *c* calcite. Spacing in Å



8 Conclusions

282

283 The complex study of structural and spectral properties of minerals in carbonate
 284 nodules evidences on microbial involvement in the genesis of studied natural and
 285 laboratory grown samples.

286 From the results obtained, one can suggest the following conclusions.
 287 (1) Studied natural nodule, as well as surrounding rocks, was not subjected to
 288 significant regional metamorphization over time after sedimentation. This is evi-
 289 denced by the presence of stable paramagnetic radiation centers in the crystal
 290 lattices of minerals forming nodules and host rocks, as well as by the presence of

Table 3 The results of XRD analysis of crystalline material precipitated by the bacterial isolates

No.	No. of sample	Content	Cell parameters	
			a, Å	c, Å
1	1–2a	Calcite	4.9810 (0.0012)	17.0367 (0.0081)
2	1–2b	Calcite	4.9784 (0.0010)	17.0324 (0.0146)
3	1–3	Calcite	4.9805 (0.0005)	17.0158 (0.0040)
4	1–4	Calcite	4.9817 (0.0009)	16.9963 (0.0082)
5	1–5	Calcite		
6	1–6	Calcite	4.9816 (0.0007)	17.0237 (0.0103)
7	2–2	Calcite	4.9763 (0.0012)	17.0529 (0.0201)
8	2–5	Calcite		
9	2–6	Calcite	4.9800 (0.0007)	17.0086 (0.0052)
10	2–7	Calcite		
11	A	Calcite	4.9808	17.0295
11	1–6-liquid	Calcite, halite	4.9816 (0.0009)	16.9952 (0.0075)
12	Control	Halite		

291 animal protein (collagen) residues in fossil OM of low metamorphization stage.
 292 (2) Similarity in crystal lattice defects for both the dolomite in nodules and host
 293 rocks confirms their formation during synsedimentary early diagenesis; (3) Since
 294 the rocks nearby sampling areas are depleted in fossil macrofauna, one can assume
 295 that the fossilized remains of animal protein occurred as a result of bacterial activity,
 296 while nodules themselves are the lithified microbial constructions. Findings of fossil
 297 bacteria additionally support this suggestion. (4) Experimental laboratory-scale
 298 modeling of natural carbonate deposition by microbial communities confirms that
 299 bacteria can promote nodules formation.

300 **Acknowledgements** Some of the study was conducted with the support of a subsidy allocated to
 301 the Kazan Federal University for state assignment in the sphere of scientific activities (Project
 302 No. 14–69) and Program of UB RAS 15-18-5-49.

303 Reference

- 304 Antipchuk AF (1979) Microbiological control in ponds. M. Food Industry
 305 Antoshkina AI (2012) Bacterial lithogenesis. In: Obzor konceptual'nykh problem litologii. In: A
 306 Review of Conceptual Problems of Lithology, Moscow: GEOS, pp 89–105
 307 Berner RA (1971) Bacterial processes effecting the precipitation of calcium carbonate in
 308 sediments. Johns Hopkins Univ Stud Geol 19:247–251
 309 Bischoff WD, Bishop FC, Mackenzie FT (1983) Biogenically produced magnesian calcite:
 310 inhomogeneities in chemical and physical properties comparison with synthetic phases. Am
 311 Mineral 68:1183–1188
 312 Conard J (1984) EPR in fossil carbonaceous materials. In: Petrakis L, Fraissard JP (eds) Magnetic
 313 resonance. Introduction. D. Reidel Publishing Company, Hingham, pp 441–459

- 314 Danielli HMC, Edington MA (1983) Bacterial calcification in limestone caves. *Geomicrobiol J*
315 3:1–15
- 316 De Craen M, Swennen R, Keppens EM, Macaulay CI, Kiriakoulakis K (1999) Bacterially
317 mediated formation of carbonate concretions in the Oligocene Boom Clay of northern
318 Belgium. *J Sediment Res* 69(5):1098–1106
- 319 *Geology of Near-Kazan region (2007) Guidebook for field student geological practice. In:*
320 *Shevelev AI (ed) “Novoie znanie”, Kazan*
- 321 Green AC, Madgwick JC (1991) Microbial formation of manganese oxides. *Appl Environ*
322 *Microbiol* 57:1114–1120
- 323 Khasanov RR, Galeev AA (2008) Evolution of sin-genetic organic material in Paleozoic deposits
324 of central part of Volga-Ural antecline. *Science. Proceedings of Kazan University. Series of*
325 *Natural Sciences*, vol 150, 3:152–161
- 326 Korolev EA, Khuzin IA, Galeev AA, Leonova LV (2014) Epigenetic transformation of dolomite
327 rocks under the influence of hydrocarbonaceous fluids (by the example of Syukeevskoe
328 bituminous deposit). *Geol Oil Gas* 5:28–32
- 329 Mason-Williams MA (1969) Microorganisms in relation to food and energy sources in caves. *Proc*
330 *Br Speleol Assoc* 4:69–74
- 331 Murav'yev FA (2007) Lithological-mineralogical characterization of Permian marking calcareous
332 horizons in Tatarstan. PhD thesis. Kazan
- 333 Paquette J, Reeder RJ (1990) Single-crystal X-ray structure refinements of two biogenic magnesian
334 calcite crystals. *Am Mineral* 75:1151–1158
- 335 Raiswell R (1976) The microbiological formation of carbonate concretions in the Upper Lias of
336 NE England. *Chem Geol* 18:227–244
- 337 Skinner HCW, Fitzpatrick RW (eds) (1992) *Biomineralization processes of iron and*
338 *manganese-modern and ancient environments. CATENA, (Supplement 21)*
- 339 Soroka EI, Leonova LV, Galeev AA, Gulyaeva TY (2007) EPR properties of organic component
340 of some high-aluminous rocks of Urals. *Lithosphere* 4:125–128
- 341 Stocks-Fischer Sh, Galinat JK, Bang SS (1999) Microbiological precipitation of CaCO₃. *Soil Biol*
342 *Biochem* 31:1563–1571
- 343 Strakhov NM (1962) *Foundation of lithogenesis. vol 2*
- 344 Tazaki K (2000) Formation of banded iron-manganese structures by natural microbial
345 communities. *Clays Clay Miner* 48(5):511–520
- 346 Votyakov SL, Galeev AA, Leonova LV, Galakhova OL, Il'inykh AS (2005) EPR as method of
347 investigation of organic component at biogenic calcareous rocks (Riphean
348 stromatolite-containing rocks from South Urals as an example). *Yearbook, Ekaterinburg,*
349 *pp 39–47*
- 350 Wei L, Li-Ping L, Peng-Peng Zh, Long C, Long-Jiang Y, Shi-Yun J (2011) Calcite precipitation
351 induced by bacteria and bacterially produced carbonic anhydrase. *Res Art Curr Sci* 100
352 (4):502–508